Available online at www.sciencedirect.com
SCIENCE DIRECT®
Geochimica et Cosmochimica Acta 70 (2006) 1172–1187
Geochimica
www.elsevier.com/locate/gca

Influence of physiology and climate on δD of leaf wax *n*-alkanes from C_3 and C_4 grasses

Francesca A. Smith *, Katherine H. Freeman

Department of Geosciences, Pennsylvania State University, 542 Deike Building, University Park, PA 16802, USA

Received 5 May 2005; accepted in revised form 4 November 2005

Abstract

We measured hydrogen isotope compositions (δD) of high-molecular-weight *n*-alkanes (C_{27}–C_{33}) from grasses grown in greenhouses and collected from the US Great Plains. In both cases, *n*-alkanes from C_4 grasses are enriched in D by more than 20‰ relative to those from C_3 grasses. The apparent enrichment factor ($\varepsilon_{C_{29}\text{-GW}}$) between C_{29} *n*-alkane and greenhouse water is -165 ± 12‰ for C_3 grasses and -140 ± 15‰ for C_4 grasses. For samples from the Great Plains, δD values of C_{29} *n*-alkanes range from -280 to -136‰, with values for C_4 grasses ca. 21‰ more positive than those for C_3 grasses from the same site. Differences in C_3 and C_4 grass *n*-alkane δD values are consistent with the shorter interveinal distance in C_4 grass leaves, and greater back-diffusion of enriched water from stomata to veins, than in C_3 grass leaves. Great Plains' grass *n*-alkane isotopic ratios largely reflect precipitation δD values. However, the offset or apparent fractionation between *n*-alkanes and precipitation is not uniform and varies with annual precipitation and relative humidity, suggesting climatic controls on lipid δD values. The dryer sites exhibit smaller absolute apparent fractionation indicative of D-enrichment of source waters through transpiration and/or soil evaporation. To explore the relationship between climate and *n*-alkane δD values, we develop three models. (1) The 'direct analog' model estimates $\delta D_{C_{29}}$ values simply by applying the apparent enrichment factors, $\varepsilon_{C_{29}\text{-GW}}$, observed in greenhouse grasses to precipitation δD values from the Great Plains. (2) The 'leaf-water' model uses a Craig–Gordon model to estimate transpirational D-enrichment for both greenhouse and field sites. The transpiration-corrected enrichment factors between C_{29} and bulk leaf-water, $\varepsilon_{C_{29}\text{-GW}}$, calculated from the greenhouse samples (-181‰ for C_3 and -157‰ for C_4) are applied to estimate $\delta D_{C_{29}}$ values relative to modeled bulk leaf-water δD values. (3) The 'soil- and leaf-water' model estimates the combined effects of soil evaporation, modeled by analogy with a flow-through lake, and transpiration on $\delta D_{C_{29}}$ values. Predictions improve with the addition of the explicit consideration of transpiration and soil evaporation, indicating that they are both important processes in determining plant lipid δD values. D-enrichment caused by these evaporative processes is controlled by relative humidity, suggesting that important climatic information is recorded in leaf wax *n*-alkane δD values. Calibration studies such as this one provide a baseline for future studies of plant-water–deuterium systematics and form the foundation for interpretation of plant wax hydrogen isotope ratios as a paleo-aridity proxy.

1. Introduction

Hydrogen isotope ratios (δD) of individual plant lipids hold great potential for reconstructing past terrestrial hydrologic conditions and climate. The hydrogen in plant tissues derives ultimately from environmental waters, which have δD ratios that are related to temperature, weather patterns, and hydrologic balance (Craig and Gordon, 1965; Gonfiantini, 1986; Rozanski et al., 1993; Gat, 1996; Dawson et al., 1998). Plant-water composition is further modified within the plant through transpiration which is also directly related to climate (Dawson et al., 2002). Recent studies have examined compound-specific δD records of biomarkers from modern (Xie et al., 2000; Andersen et al., 2001; Huang et al., 2001, 2002, 2004; Sauer et al., 2001; Yang and Huang, 2003; Sachse et al., 2004b) and ancient sediments (Xie et al., 2000; Andersen et al., 2001;

* Corresponding author. Fax: +1 814 863 7823.
E-mail address: cesca@earth.northwestern.edu (F.A. Smith).

0016-7037/$ - see front matter © 2005 Elsevier Inc. All rights reserved.
doi:10.1016/j.gca.2005.11.006

Huang et al., 2001, 2002, 2004; Sauer et al., 2001; Yang and Huang, 2003; Sachse et al., 2004a; Schefuß et al., 2005) and their relationship to surface water δD values and climate.

Significant contributors to these sedimentary records include high-molecular weight, odd-carbon numbered (C_{27}–C_{33}) straight-chain hydrocarbons (*n*-alkanes) that are distinctive constituents of vascular plant leaf waxes (Eglinton and Hamilton, 1967). The abundance and carbon isotope signature of these *n*-alkanes have been used to quantify and characterize terrestrial plant contributions to ancient sediments and soils (Yamada and Ishiwatari, 1999; Huang et al., 2000; Zhao et al., 2000; Freeman and Colarusso, 2001). Because all hydrogen atoms in *n*-alkanes are covalently bound to carbon atoms, they have very slow rates of exchange as demonstrated by primary signatures in thermally immature sediments of Cretaceous and younger age (Schimmelmann et al., 1999; Andersen et al., 2001; Yang and Huang, 2003; Pedentchouk, 2004; Sessions et al., 2004). Hydrogen isotope ratios of other plant biomolecules such as cellulose and saponifiable lipids have long been recognized as natural tracers for both intrinsic, plant physiological processes and extrinsic, environmental conditions (Epstein et al., 1976; Northfelt et al., 1981; Yapp and Epstein, 1982; Sternberg et al., 1984; White et al., 1985; Sternberg, 1988; Dawson et al., 2002; Shu et al., 2005). More recently, hydrogen isotope ratios of leaf wax *n*-alkanes from modern lake sediments have been shown to have a strong linear relationship with meteoric water values (Sachse et al., 2004b). However, the specific roles of plant type, physiology, and climate in determining the δD signatures of leaf wax *n*-alkanes in modern plants has only begun to be examined (Chikaraishi and Naraoka, 2003; Chikaraishi et al., 2004; Bi et al., 2005).

Compound-specific hydrogen isotope analyses can eliminate the confounding effects resulting from the mixing of various compound classes and inputs from multiple types of source organisms to sedimentary records. Even within a single organism, different compounds can have remarkably different δD values. For example, within leaves of a carrot plant, the δD value of C_{31} *n*-alkane was more than 250‰ more positive than that of phytol (Sessions et al., 1999). Significant isotopic variation can also be observed among cohabiting species. Variation of up to nearly 90‰ has been observed in C_{29} *n*-alkane in different C_3 angiosperm taxa grown in the same area (Chikaraishi and Naraoka, 2003). Thus, interpretation of leaf wax *n*-alkane δD records from sediments requires systematic studies of the physiological and environmental controls on these signatures in modern plants.

Leaf architecture associated with specific photosynthetic pathways and growth form (e.g., grass versus tree) is an intrinsic factor that is likely to influence the hydrogen isotope ratios of plant compounds. Previous studies on δD ratios of plant lipids have compared C_4 grasses to C_3 trees, shrubs, and herbs (Sternberg et al., 1984; Ziegler, 1989; Chikaraishi and Naraoka, 2003) and the results disagree about whether and how δD ratios differ between C_3 and C_4 plants. This disagreement most likely results from comparing plants with different growth forms and disregarding the effects of climate. Grasses are monocotyledonous, and have long parallel veins in their leaves, whereas dicotyledonous angiosperm herbs, shrubs, and trees have branching veins. This fundamental difference in veinal structure strongly influences the oxygen isotope ratio of leaf-water and -cellulose (Helliker and Ehleringer, 2000, 2002a) and could also play a large role in hydrogen isotope ratios of leaf-water and plant tissues.

Environmental factors that affect the hydrogen isotope ratio of plant compounds can be considered in two stages: (1) the initial hydrogen isotope ratio of water entering the soil–plant system as precipitation and (2) subsequent modification of the isotope ratio of that water though evaporation from leaves (transpiration) and evaporation from soils. In North America, precipitation δD values vary spatially and seasonally with more positive values generally at lower latitudes and during the summertime (Craig and Gordon, 1965; Rozanski et al., 1993; Gat, 1996). The evaporative conditions at the soil and leaf surfaces will vary with climatic conditions including temperature, relative humidity and windspeed (Larcher, 1995). Because evaporation (from both soils and leaves) always leads to D-enrichment of leaf-water, enrichment factors calculated between lipids and precipitation, $\varepsilon_{\text{lipid-precip}}$, underestimate biochemical fractionation. The confounding spread in published $\varepsilon_{\text{lipid-precip}}$ and δD values may reflect the lack of constraints on climatic influences on evaporation from soils and leaves.

In this paper, we present results from an initial examination of hydrogen isotope ratios of individual *n*-alkanes from grasses in relation to photosynthetic type (C_3 or C_4), source water δD values and climate. By restricting the analysis to grasses, we avoid the added complexity of comparing dicots to monocots. In addition, because grasslands generally occur in semi-arid areas where groundwater is unavailable to grass roots (Boutton et al., 1999; Welker, 2000), we focus solely on soil- and plant-water signals. In an effort to examine intrinsic, physiological effects and extrinsic, environmental factors, we sample grasses grown in a greenhouse and wild grasses from the Great Plains. The greenhouse study provides a controlled environment in which C_3 and C_4 grasses were grown in identical conditions using the same source water of known isotopic composition. In contrast, the grasses from the Great Plains grew under natural conditions with a range of meteoric water δD values, and a range of climatic conditions. We explicitly examine the effects of climate on transpiration and soil evaporation through the application of a series of isotopic models. The combined greenhouse and field sample sets allow us to address the questions: (1) Do δD values of *n*-alkanes from C_3 and C_4 grasses grown side by side differ? (2) Are spatial variations in meteoric water δD values reflected in *n*-alkane δD values of grasses? and (3) How are *n*-alkane δD values influenced by climate?

2. Materials and methods

2.1. Greenhouse grasses

We sampled above-ground tissue from C_3 and C_4 grasses grown in the same greenhouse at the Pennsylvania State University, under identical temperature and relative humidity conditions. The average relative humidity for the month preceding sampling was 52% and the average temperature was 20 °C. Samples represent 5 C_3 and 5 C_4 species (Table 1). All plants were grown either in large well-drained benches or large well-drained pots to avoid evaporative enrichment of standing water. The only exception is 'Hard fescue 1' that was grown in a small pot resting on a drain pan. 'Hard fescue 2,' in contrast, was grown in a large bench. These samples allow for comparison of the effects of different pot conditions on the same species. The plants were watered regularly using tap water. The tap water was collected throughout the summer and the hydrogen and oxygen isotope ratio of the water was measured at the Stable Isotope Laboratory at INSTAAR, University of Colorado, Boulder. Hydrogen and oxygen isotope ratios were measured using a uranium reduction furnace (Vaughn et al., 1998) and CO_2 equilibration system (Epstein and

Table 1
Greenhouse grass *n*-alkane δD values (‰ VSMOW) and apparent enrichment factors relative to greenhouse water (−61.3‰)

Common name	Latin name	Type	*n*-Alkane chain length						$\varepsilon_{C_{29}\text{-GW}}$
			C_{25}	C_{27}	C_{29}	C_{31}	C_{33}	C_{35}	
Hard fescue 1	*Festuca longifolia* L.	C_3			−223	−217	−204		−172
Hard fescue 2	*Festuca longifolia* L.	C_3			−232	−228	−218		−182
Timothy	*Phleum pretense*	C_3	−208	−203	−196	−202	−192		−143
Smooth brome	*Bromis inermis*	C_3			−223	−235			−172
Ryegrass	*Lolium multiflorum Lam.*	C_3	−161	−167	−200	−207	−195		−148
Tall fescue	*Festuca arundinacea Schreb.*	C_3			−222	−233	−212		−172
C_3 average ± 95% CI:					−216 ± 12	−220 ± 11	−204 ± 10		−165 ± 12
St. Augustine	*Stenotaphrum secundatum*	C_4		−172	−186	−193	−193	−166	−133
Bahia grass	*Paspalum notatum flugge*	C_4				−162	−169	−165	
Zoysia	*Zoysia japonica Steud*	C_4	−160	−159	−176	−176	−187	−167	−122
Switchgrass	*Panicum virgatum*	C_4		−195	−203	−198			−151
Little Bluestem	*Schizachyrium scoparium*	C_4		−182	−207	−209			−155
C_4 average ± 95% CI:				−177 ± 15	−193 ± 14	−188 ± 16	−183 ± 14	−166 ± 1	−140 ± 15

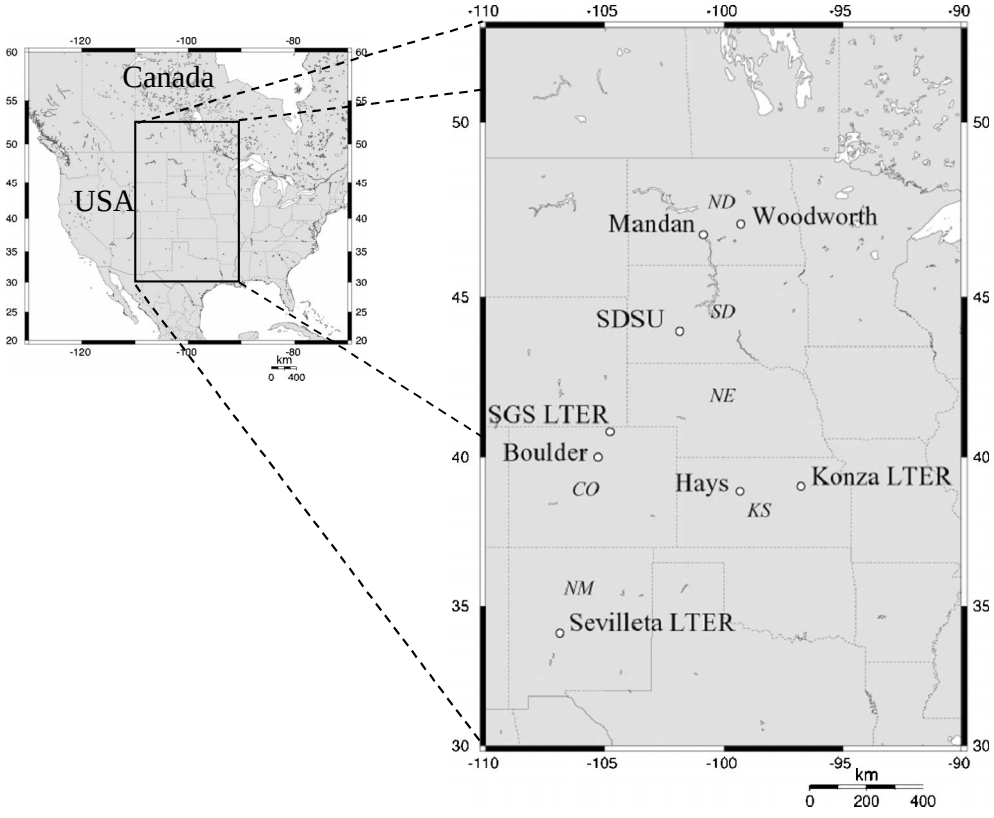

Fig. 1. Collection sites for grasses. Site location information in Table 2.

Mayeda, 1953) respectively, each coupled with a Micromass SIRA Series II.

2.2. Grasses from the US Great Plains

Above-ground tissues of grasses (*Poaceae*) were collected as part of a previous study on carbon isotopes (Smith and White, 2004) from eight sites in the US Great Plains (Fig. 1). Because of the potential for isotopic fractionation in leaf-water along the length of the blade (Helliker and Ehleringer, 2000), entire leaves were sampled along with stems. Both C_3 and C_4 grasses were collected at each site with a total of 18 C_3 and 22 C_4 grass samples representing 18 different species (Table 2). The sites span a large geographic area and consequently a large range in meteoric water δD values. River waters values from these sites range from −45 to −115‰ (Kendall and Coplen, 2001) and estimated July precipitation

Table 2
δD values (‰ VSMOW) for *n*-alkanes from grasses from the Great Plains and site information

Latin name	Common name	Photosynthesis	*n*-Alkane chain length						
			C_{23}	C_{25}	C_{27}	C_{29}	C_{31}	C_{33}	C_{35}
WDW: Northern Prairie Wildlife Research Center, Woodworth, ND (47°09′N, 99°18′W)									
Stipa viridula	Green needlegrass	C_3				−232	−257	−249	
Poa pratensis	Kentucky bluegrass	C_3			−227	−247	−254	−244	
Stipa comata	Needleandthread	C_3				−231	−238		
Bromus inermis	Smooth brome	C_3				−275	−280		
Andropogon gerardii	Big bluestem	C_4			−219	−225	−234	−221	
Schizachyrium scoparium	Little bluestem	C_4				−223	−224		
MNDN: Northern Great Plains Research Lab, USDA, Mandan, ND (46°50′N, 100°55′W)									
Stipa viridula	Green needlegrass	C_3			−235	−239	−254	−235	
Stipa comata	Needleandthread	C_3			−244	−222	−218	−219	−221
Agropyron smithii	Western wheatgrass	C_3			−248	−251	−249	−253	
Bouteloua gracilis	Blue grama	C_4			−208	−220	−232	−222	
Schizachyrium scoparium	Little bluestem	C_4	−232	−230	−230	−228	−230		
Calamovilfa longifolia	Prairie sandreed	C_4		−228	−230	−216	−213		
SDSU: Cottonwood Range and Livestock Research Station, Cottonwood, SD (43°58′N, 101°52′W)									
Koeleria pyramidata	Junegrass	C_3			−262	−261	−263		
Bromus inermis	Smooth brome	C_3			−237	−238	−255		
Agropyron smithii	Western wheatgrass	C_3				−244	−246		
Buchloe dactyloides	Buffalograss	C_4			−215	−219	−209		
Schizachyrium scoparium	Little bluestem	C_4	−229	−228	−224	−233	−236	−220	
Aristida longiseta	Red threeawn	C_4				−196	−214	−233	
Bouteloua curtipendula	Sideoats grama	C_4			−220	−213	−219		
SGS: Shortgrass Steppe LTER, Nunn, CO (40°42′N, 104°47′W)									
Stipa comata	Needleandthread	C_3			−221	−210	−219	−215	
Agropyron smithii	Western wheatgrass	C_3				−214	−218		
Bouteloua gracilis	Blue grama	C_4	−161	−166	−171	−189	−211	−213	
BLDR: Cherryvale East, Boulder, CO (40°00′N, 105°16′W)									
Bromus inermis	Smooth brome	C_3				−273	−284		
Andropogon gerardii	Big bluestem	C_4	−234	−235	−234	−238	−235	−233	
Schizachyrium scoparium	Little bluestem	C_4			−235	−253	−266	−253	
KNZA: Konza Prairie LTER, near Manhattan, KS (39°12′N, 96°35′W)									
Elymus canadensis	Canada wildrye	C_3		−216	−234	−234	−230		
Poa pratensis	Kentucky bluegrass	C_3				−220	−230	−227	
Andropogon gerardii	Big bluestem	C_4		−205	−211	−205	−204	−191	
Sorghastrum nutans	Indiangrass	C_4		−204	−199	−197	−192	−176	
Schizachyrium scoparium	Little bluestem	C_4		−187	−193	−196	−207	−199	
HAYS: Fort Hays College Farm, Hays, KS (38°52′N, 99°20′W)									
Agropyron smithii	Western wheatgrass	C_3				−211	−207		
Andropogon gerardii	Big bluestem	C_4		−207	−212	−213	−213		
Sorghastrum nutans	Indiangrass	C_4		−191	−203	−196	−197		
Panicum virgatum	Switchgrass	C_4			−205	−212	−205		
SVL: Sevilleta LTER, Socorro County, NM (34°05′N, 106°53′W)									
Oryzopsis hymenoides	Indian ricegrass	C_3			−193	−187	−189		
Stipa comata (*newmexicanus*)	Needleandthread	C_3				−167	−174		
Bouteloua eriopoda	Black grama	C_4				−136	−155	−165	
Bouteloua gracilis	Blue grama	C_4		−176	−180	−190	−210	−207	

values range from −54 to −86‰ (www.waterisotopes.org; Bowen and Wilkinson, 2002; Bowen and Revenaugh, 2003). Annual rainfall ranges from 233 to 718 mm across the study sites (State Climatological Summaries from http://nndc.noaa.gov). Ecosystem types include shortgrass steppe, tallgrass prairie, mixed prairie, and desert grasslands (Coupland, 1992) reflecting the widely varying climates across the Great Plains of North America.

2.3. Lipid extraction

Great Plains grasses were dried at room temperature in paper bags, and greenhouse grasses were dried in paper bags at 70 °C for 2–4 days. Dried plant material was cut into pieces approximately 1 cm in length and 1–2 g of each sample was used for extraction. Lipids were extracted using repeated (3×) ultrasonication in dichloromethane/methanol (93/7, v/v) for 15 min (Collister et al., 1994). The total lipid extract was then separated into polarity fractions using short columns filled with approximately 3 g of activated silica gel (70–230 mesh). The hydrocarbon fraction was eluted using hexane (10 mL) and a polar fraction was eluted using dichloromethane/methanol (1/1, v/v) and archived. The *n*-alkanes were identified through mass spectra, molecular ion mass, retention time, and comparison with authentic standards (“Mixture A” from A. Schimmelmann) using an Agilent 6890 gas chromatograph coupled to an Agilent 5972 quadropole mass spectrometer. The GC oven program increased from 60 °C (held for 1 min) to 320 °C at 6 °C/min, and was held at 320 °C for 20 min.

2.4. Compound-specific deuterium analyses

Hydrogen-isotope ratios of individual *n*-alkanes were measured on a Thermo Finnigan Delta Plus XP with a gas chromatograph combustion interface (GCC) with a high-temperature pyrolysis furnace (1400 °C) coupled with an Agilent 6890A GC–MS (Burgoyne and Hayes, 1998; Hilkert et al., 1999). The GC was programmed from 60 °C (held for 1 min) to 170 °C at 15 °C/min and then to 320 °C at 5 °C/min, and held for 20 min. The samples were analyzed in three batches separated by several months. The average H_3 factor (±SD) measured daily during each 2–3 week period of measurement was 8.696 ± 0.096 ppm, 9.021 ± 0.094 ppm, and 7.914 ± 0.070 ppm (Sessions et al., 2001). Isotope ratios were calculated relative to a co-injected standard containing C_{14} *n*-alkane to condition the furnace and androstane, squalane, and C_{41} *n*-alkane as compounds with known isotopic values. The isotope ratios for androstane (−256.4‰), squalane (−169.9‰), and nC_{41} (−205.7‰) were determined relative to external standards using off-line pyrolysis (measurements by A. Schimmelmann). Sample values were calculated relative to the androstane standard peak, except in the rare case of co-elution or high background in the androstane window. In those cases, sample values were determined relative to squalane. Each sample was run at least twice and the standard deviation of replicate measurements for individual *n*-alkanes was generally less than 5‰, with an average of 2.0‰ and 2.2‰ for C_{29} and C_{31}, respectively. In most sample runs, squalane and nC_{41} were treated as unknowns. The average hydrogen isotope value for squalane co-injected with 108 samples was −170.9‰ with a standard deviation of 3.1‰, which corresponds well with the off-line value of −169.9‰. The average value for nC_{41} co-injected with 63 samples was −207.7‰ with a standard deviation of 4.0‰, which compares well with the off-line value of −205.7‰. We also determined instrument performance daily by measuring a suite of C_{16} to C_{30} *n*-alkanes (“Mixture A” from A. Schimmelmann) with a co-injected standard with nC_{14}, androstane, squalane, and nC_{41}. The standard deviation ranges from 1.3 to 5‰ with an average of 2.2‰ for 20 replicate measurements of the 15 *n*-alkanes in Mixture A. A conservative estimate of instrument precision is ±5‰ or better.

3. Results

High-molecular weight, odd-carbon-numbered *n*-alkanes in greenhouse and field grass samples ranged from C_{23} to C_{35}, with the most abundant being C_{27}, C_{29}, and C_{31}. The hydrogen isotope ratios of the most abundant *n*-alkanes are presented in Tables 1 and 2 and, in all but one case, these include C_{29} and C_{31}. Hydrogen isotope ratios of C_{29} and C_{31} *n*-alkanes are strongly correlated ($r = 0.951$, $n = 48$). The geometric mean regression of $\delta D_{C_{29}}$ and $\delta D_{C_{31}}$ has a slope of 1.029 and an intercept of 2.4‰, which is within measurement precision of a 0-intercept. As a result, the subsequent discussion focuses on the results for C_{29} *n*-alkanes, although data for all compounds are provided.

In the greenhouse samples, *n*-alkanes (C_{25} to C_{31}) from C_4 grasses have more positive δD values than those from C_3 grasses, with an average difference of 22 ± 8‰ (95% CI). The C_{29} *n*-alkane average values are -216 ± 12‰ (95% CI) for C_3 grasses and -193 ± 14‰ (95% CI) for C_4 grasses (Table 1). The difference between the mean $\delta D_{C_{29}}$ for C_3 and C_4 grasses is 23‰ and is statistically significant at the 95% level (Student’s *t* test, *p* value = 0.039). Drainage conditions seemed to have an effect as illustrated by Hard fescue 1, which was grown in a small pot resting in a drain pan, and has δD values that are 9–14‰ more positive than the same species, Hard fescue 2, grown in a well-drained bench. The standing water in the drain pan may have experienced evaporation and lead to more positive *n*-alkane δD values. Hard fescue 1 was the only sample exposed to standing water.

Greenhouse water was sampled weekly from mid May through June and exhibited constant hydrogen and oxygen isotope ratios. The water δD value was -61.3 ± 0.5‰ (95% CI, $n = 7$) and $\delta^{18}O$ value of -9.21 ± 0.03‰ (95%

CI, $n = 9$). The apparent enrichment factor between C_{29} *n*-alkane and greenhouse water (GW), $\varepsilon_{C_{29}\text{-GW}}$, is defined as

$$\varepsilon_{C_{29}\text{-GW}} = (R_{C_{29}}/R_{GW} - 1) \times 1000‰, \quad (1)$$

where $R = D/H$. The average $\varepsilon_{C_{29}\text{-GW}}$ values are $-165 \pm 12‰$ for C_3 grasses and $-140 \pm 15‰$ (95% CI) for C_4 grasses. These are termed "apparent" enrichment factors because they represent the net fractionation between the greenhouse water and *n*-alkane, which is the result of D-depletion due to biochemical fractionation as well as any evaporative D-enrichment due to transpiration and evaporation from soils.

Hydrogen isotope ratios of *n*-alkanes from Great Plains grasses span over 140‰ and range from −280‰ to −136‰ (Table 2). The values vary from site to site as illustrated in Fig. 2 for C_{29} *n*-alkanes. With few exceptions, C_4 grasses have more positive *n*-alkane δD values than C_3 grasses grown at the same site (Fig. 2, Table 2). On average, C_{29} *n*-alkane δD values for C_4 grasses are $21 \pm 6‰$ (95% CI) more positive than for C_3 grasses from a given site (Table 3).

4. Discussion

4.1. Comparison of C_3 and C_4 grasses

n-Alkane δD values for C_4 grasses are ca. 20‰ more positive than for C_3 grasses in both the environmentally controlled greenhouse experiment and in the naturally variable Great Plains samples (Tables 1 and 3). C_3 and C_4 grasses are fundamentally different with respect to growing season, leaf anatomy, and biochemistry, suggesting several possible reasons for the observed isotopic differences. For example, grasses that perform C_3 photosynthesis are 'cool season' grasses, and at a given site often grow earlier than the 'warm season' (C_4) grasses. Precipitation δD values are more negative during cooler months, and more positive during warmer months (Rozanski et al., 1993) and can vary by over 80‰ between May and August in the Great Plains (Harvey and Welker, 2000). If C_4 grasses sampled exclusively warm season precipitation, they should have more positive δD values than C_3 grasses. Although this is what we observe, we also observe the same difference in the C_3

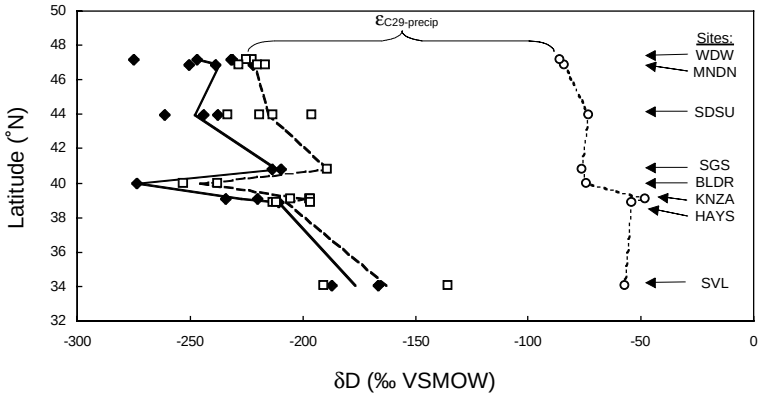

Fig. 2. Hydrogen isotope ratios of C_{29} *n*-alkane from C_3 grasses (solid diamonds) and C_4 grasses (open squares) and annual precipitation (open circles). Average C_{29} values for each site connected with solid lines for C_3 and dashed lines for C_4. Annual precipitation values estimated using the Online Isotopes in Precipitation Calculator at http://www.waterisotopes.org/. Apparent enrichment factor is a measure of the difference between $\delta D_{C_{29}}$ and δD_{precip}, $\varepsilon_{C_{29}\text{-precip}} = (R_{C_{29}}/R_{precip} - 1) \times 1000‰$; R = D/H.

Table 3
Average C_3 and C_4 C_{29} *n*-alkane δD values for each site in the Great Plains, apparent enrichment factors relative to precipitation, and 'direct analog' model values (‰ VSMOW)

Site	C_3 measured		C_4 measured		$C_4 - C_3$ difference	δD_{precip}[a]	$\varepsilon_{C_{29}\text{-precip}}$	$\varepsilon_{C_{29}\text{-precip}}$	Direct analog	
	$\delta D_{C_{29}}$	SD (*n*)	$\delta D_{C_{29}}$	SD (*n*)			C_3	C_4	$\delta D_{C_{29}} C_3$	$\delta D_{C_{29}} C_4$
WDW	−246	21 (4)	−224	1 (2)	23	−86	−175	−151	−237	−214
MNDN	−237	14 (3)	−222	6 (3)	15	−84	−167	−151	−235	−212
SDSU	−248	12 (3)	−215	16 (4)	33	−73	−189	−153	−226	−203
SGS	−212	3 (2)	−189	0 (2)	23	−76	−147	−122	−228	−205
BLDR	−273	(1)	−245	11 (2)	28	−74	−215	−184	−227	−204
KNZA	−227	10 (2)	−199	5 (3)	28	−48	−188	−159	−205	−181
HAYS	−211	(1)	−207	9 (3)	4	−54	−166	−162	−210	−186
SVL	−177	14 (2)	−163	39 (2)	14	−57	−127	−112	−213	−189
Average ± 95% CI:					21 ± 6		−166 ± 16[b]	−144 ± 14[b]		

[a] δD of annual precipitation estimated using OIPC, at www.waterisotopes.org.
[b] Excluding BLDR.

and C_4 grasses grown in the greenhouse using isotopically identical source water. Thus, seasonal variation in precipitation δD values does not appear to leave a signature on the leaf wax δD values. This indicates that the δD values of soil waters used by the Great Plains grasses are time-averaged and do not preserve seasonal variations as observed previously (Tang and Feng, 2001). Alternatively, or in addition, *n*-alkane production could be either: (1) stimulated and synchronized by environmental conditions in both C_3 and C_4 grasses or (2) continuous over the course of the growing season, leaving an isotopic signature of the latest growth.

The greenhouse results suggest that the underlying cause for the difference between C_3 and C_4 δD values must be intrinsic to the plants and result from either biochemical or anatomical properties. Previous work by Helliker and Ehleringer identified a 4–5‰ enrichment in ^{18}O of leaf-water of C_4 relative to C_3 grasses, which they attribute to differences in leaf anatomy (Helliker and Ehleringer, 2000). Sub-sampling along the length of an individual leaf reveals a progressive enrichment in ^{18}O of leaf-water from stem to tip of on the order of 50‰ (Helliker and Ehleringer, 2000). They hypothesize that this progressive stem-to-tip enrichment is due to evaporation through stomata and back-mixing of enriched stomatal water with vein water. The degree of mixing is controlled by the back-diffusion path length, which is a function of the distance between the veins. The interveinal distance in C_4 grasses is shorter than in C_3 grasses, leading to greater back-diffusion of isotopically enriched stomatal water, resulting in more positive leaf-water and -cellulose $\delta^{18}O$ values in C_4 grasses (Helliker and Ehleringer, 2000, 2002a; Farquhar and Gan, 2003). The same mechanism could also be affecting the hydrogen isotope ratio of leaf waxes, assuming that they derive their hydrogen from leaf-water. Because transpiration is simply evaporation, the expected slope of the δD–$\delta^{18}O$ relationship is often approximately 5 (Craig et al., 1963). This differs from the slope of 8 observed for the Global Meteoric Water Line (Craig, 1961; Dansgaard, 1964) which reflects the near-equilibrium condensation of water at near-saturation conditions, and leads to a slope close to the ratio of the equilibrium fractionation factors for δD and $\delta^{18}O$. Evaporation, on the other hand, is a non-equilibrium process that occurs at less than saturation and imparts a proportionally greater kinetic isotope effect on ^{18}O than on D and thereby reduces the δD–$\delta^{18}O$ slope (Ingraham, 1998). Thus, the observed difference of 20‰ in hydrogen isotope ratios in *n*-alkanes from C_3 and C_4 grasses is of comparable magnitude to the 4–5‰ difference in $\delta^{18}O_{leaf\text{-}water}$ values observed by Helliker and Ehleringer (2000).

The apparent enrichment factors calculated for the greenhouse grasses (C_3 $\varepsilon_{C_{29}\text{-}GW}$, -165 ± 12‰; C_4 $\varepsilon_{C_{29}\text{-}GW}$, -140 ± 15‰; ±95% CI) contrast with a previous study in which average $\varepsilon_{lipid\text{–}water}$ values for *n*-alkanes were found to be more positive for C_3 (-117 ± 27‰, SD) than for C_4 angiosperms (-132 ± 12‰, SD) (Chikaraishi and Naraoka, 2003). In their study, however, Chikaraishi and Naraoka (2003) compare C_3 dicots (herbs, shrubs, and trees) to C_4 monocots (grasses). Here, we compare C_3 and C_4 grasses and find C_4 grasses have more positive $\varepsilon_{lipid\text{–}water}$ values than C_3 grasses (Table 1). Additional evidence for $\varepsilon_{lipid\text{–}water}$ values for C_3 dicots can be derived from Sachse et al. (2004b) who calculate the enrichment factor between δD of C_{29} *n*-alkanes from lake sediments relative to meteoric waters as -130 ± 8‰ (SD). The lakes represent a latitudinal transect across Europe, and should be dominated primarily by C_3 dicots. The data from these three studies suggest some general patterns: (1) grasses appear to have more negative $\varepsilon_{lipid\text{–}water}$ values than dicots and (2) $\varepsilon_{lipid\text{–}water}$ values are most negative for C_3 grasses, intermediate for C_4 grasses, and least negative for C_3 dicots. Therefore, photosynthetic pathway (C_3 or C_4) is not the determining factor in hydrogen isotope fractionation in *n*-alkanes. Instead, leaf architecture (e.g., interveinal distance, parallel versus branching veins) and overall plant water-balance seems to be more important in determining $\varepsilon_{lipid\text{–}water}$ values through transpirational enrichment. Many grasses are adapted to semi-arid conditions and have a higher water-use efficiency and a lower transpiration rate than many dicots (Larcher, 1995). Water-use efficiency of C_4 grasses has been shown to be 1.5- to 2-fold higher than C_3 trees in a West African savanna (Simioni et al., 2004). Such differences in plant–water relations may explain the larger absolute, more negative apparent fractionation observed in grasses relative to dicots.

4.2. Meteoric water δD reflected in n-alkane δD

The hydrogen isotope composition of soil waters vary to a first order with latitudinal patterns in precipitation δD values observed in North America (IAEA, 2001). Likewise, the hydrogen isotope ratio of C_{29} *n*-alkanes (Fig. 2) vary from site to site with a general trend of more negative values at higher latitudes to more positive values at lower latitudes. The three most northern sites, WDW, MNDN, and SDSU have values that are on average ~60‰ more negative than the southernmost site, SVL (Fig. 2, Table 3). The latitudinal intermediates, SGS, KNZA, and HAYS generally have intermediate values with the notable exception of BLDR, from Boulder, CO. Boulder sits directly in front of the foothills of the Rocky Mountains, and the more negative values for lipids from this site likely reflect either the effects of more negative local precipitation δD values due to greater convection, or the effect of D-depleted alpine snowmelt flowing from the mountains (Rozanski et al., 1993; Welker, 2000).

Annual precipitation δD values for each site can be estimated by interpolation of measured data using the model of Bowen and Wilkinson (2002) and Bowen and Revenaugh (2003) by way of the Online Isotopes in Precipitation Calculator (OIPC) (www.waterisotopes.org) (Table 3, Fig. 2). The δD_{precip} estimate for BLDR does not show strongly D-depleted precipitation suggesting either that the

OIPC model does not fully capture the isotopic dynamics of precipitation in the foothills of the Rocky Mountains or that the BLDR source water is dominated by precipitation from higher elevations. Overall, the δD_{precip} values show a latitudinal trend like that seen in lipids and support the conclusion that *n*-alkane δD values are primarily controlled by δD_{precip} values. However, the magnitude of the difference between the northern and southern sites is only ~30‰ in precipitation, whereas it is ~60‰ in the *n*-alkanes. This difference suggests that climate may be modifying the water used in lipid synthesis through transpiration and soil evaporation. Although these processes add to the complexity of interpreting isotopic data, they also may provide useful information about climate.

4.3. Climatic influences on n-alkane δD

Both transpiration and evaporation from soils are controlled by climate and will lead to D-enrichment in the leaf- and soil-water, respectively. The degree of enrichment relative to precipitation δD values can be related to climatic parameters. To examine potential relationships, we can exploit the fact that apparent fractionations between *n*-alkanes and precipitation are subject to evaporational effects to look for evidence of evaporation. Because $\varepsilon_{C_{29}\text{-precip}}$ measures the difference between δD_{precip} and C_{29} *n*-alkane (Fig. 2), any D-enrichment in leaf or soil waters will offset the negative fractionation associated with lipid synthesis and lead to smaller absolute, or less negative, apparent $\varepsilon_{C_{29}\text{-precip}}$ values. Thus, sites with greater evaporation from leaves and soils should also exhibit less negative $\varepsilon_{C_{29}\text{-precip}}$ values. Average $\varepsilon_{C_{29}\text{-precip}}$ values vary by 50‰ for C_4 and 60‰ for C_3 (excluding BLDR; Table 3) and show a strong relationship with annual rainfall (Fig. 3A). The sites with the lowest annual rainfall have the smallest absolute, or least negative, $\varepsilon_{C_{29}\text{-precip}}$ values. A similar relationship exists between $\varepsilon_{C_{29}\text{-precip}}$ and July relative humidity, with dryer sites having less negative $\varepsilon_{C_{29}\text{-precip}}$ values, with the notable exception of BLDR (Fig. 3B). As discussed above, BLDR is potentially strongly influenced by its proximity to the mountains. The correspondence of dryer sites and smaller absolute $\varepsilon_{C_{29}\text{-precip}}$ values suggests that transpiration and/or soil evaporation is leading to D-enrichment in the waters being used to synthesize lipids.

4.4. Modeling transpiration and soil evaporation effects

Characterizing the relationship between D-enrichment in *n*-alkanes and climatic parameters in a mechanistic way is the first step toward interpreting hydrogen isotope values in terms of climate. We compare three models of increasing complexity in which we predict $\delta D_{C_{29}}$ by using the data from the greenhouse experiments and models of the effects of climate on evaporative conditions in soils and leaves.

4.4.1. The 'direct analog' model

This model calculates $\delta D_{C_{29}}$ values by applying the observed apparent fractionations from the greenhouse grasses ($\varepsilon_{C_{29}\text{-GW}}$: −165‰ for C_3 and −140‰ for C_4) directly to annual precipitation δD values (Table 3). This simple model assumes that the conditions that lead to the fractionation observed in the greenhouse are directly analogous to those in the Great Plains. The $\varepsilon_{C_{29}\text{-GW}}$ values represent net fractionation between greenhouse water and C_{29} *n*-alkane, which is the result of both biochemical fractionation and D-enrichment resulting from transpiration and evaporation from soils. The degree of D-enrichment due to evaporation is a function of temperature, through its effect on equilibrium fractionation, and relative humidity through its effect on kinetic fractionation (Craig and Gordon, 1965). The plants in the greenhouse grew at an average temperature of 20 °C and an average relative humidity of 52% in well-watered and well-drained pots. The eight sites in the Great Plains have an average July temperature of 23.8 ± 1.7 °C (95% CI) and an average July relative humid-

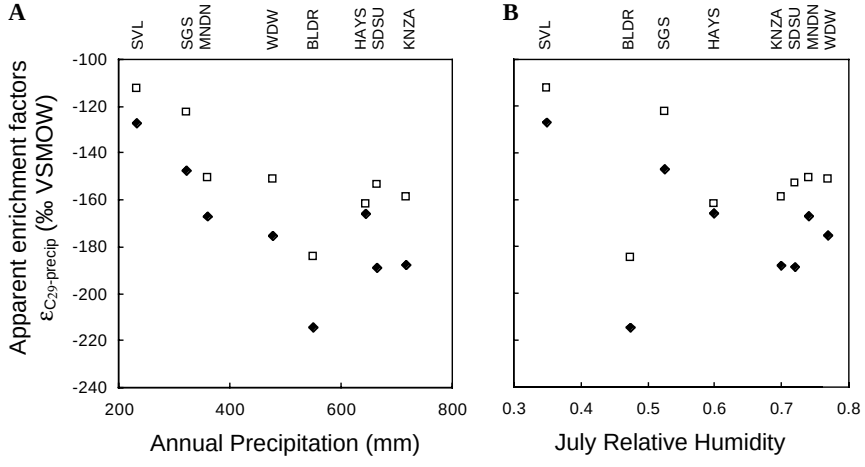

Fig. 3. Average apparent enrichment factors between C_{29} *n*-alkanes and δD_{precip}, $\varepsilon_{C_{29}\text{-precip}}$, for C_3 (solid diamonds), and C_4 (open squares) grasses from the Great Plains versus (A) average annual precipitation for 1996 and 1997 and (B) July relative humidity for each site (Table 4).

Table 4
Climate data and 'leaf-water' model calculations of C_{29} *n*-alkane δD (‰ VSMOW)

Site	Date collected	Annual precip. (mm)[a]	July rel. humidity (%)[b]	July temp. (C)[c]	α^{*}[d]	δD_{TE}	δD_{BLW}[e]	Leaf-water model C_3 $\delta D_{C_{29}}$[f]	Leaf-water model $C_4 \delta D_{C_{29}}$[f]
WDW	8/21/97	478	77	21.7	1.0824	−63	−77	−244	−222
MNDN	8/22/97	360	74	21.6	1.0826	−58	−74	−242	−220
SDSU	8/24/97	664	72	22.0	1.0821	−45	−63	−232	−210
SGS	8/29/97	323	53	23.7	1.0802	−29	−58	−229	−206
BLDR	10/8/96	551	48	21.9	1.0821	−21	−55	−226	−203
KNZA	8/11/97	718	70	25.4	1.0759	−19	−37	−211	−188
HAYS	7/15/97	644	60	27.7	1.0783	−14	−39	−213	−190
SVL	12/2/96	233	35	26.1	1.0776	7	−33	−208	−185
GreenHs[g]			52	20.0	1.0844	−11	−43		

[a] Average annual precipitation for 1996 and 1997 from state climatological summaries (http://nndc.noaa.gov).
[b] Estimated from NCEP/NCAR reanalysis (http://www.cdc.noaa.gov/Composites/).
[c] Mean July temperature from state climatological summary sites (http://nndc.noaa.gov) for July 1996 for BLDR and SVL and July 1997 for all other sites.
[d] Liquid–vapor equilibrium fractionation factor calculated using and equation of Horita and Wesolowski (1994) and July temperatures.
[e] Calculated δD of bulk leaf-water (BLW) with $f_t = 37\%$.
[f] Calculated using greenhouse derived estimates of $\varepsilon_{C_{29}\text{-BLW}}$ of −181‰ for C_3 and −157‰ for C_4.
[g] Greenhouse data used to calculate greenhouse δD_{BLW} and $\varepsilon_{C_{29}\text{-BLW}}$. Climate data for month preceding harvesting.

ity of 61 ± 10% (95% CI) (Table 4). The higher temperature and relative humidity of the Great Plains sites should lead to less D-enrichment from transpiration and soil evaporation than in the greenhouse. In contrast, the soils in the Great Plains are probably coarser and less frequently flushed than the soil used in the greenhouse, such that a greater proportion of soil-water is subject to evaporative loss. This would facilitate more D-enrichment through evaporation relative to greenhouse soils. The relative importance of these differences is difficult to judge. Therefore, as a starting point for comparison, the 'direct analog' model applies net enrichment factors and implicitly assumes that the effect of soil evaporation, transpiration, and biochemical fractionation in the greenhouse is the same as in the Great Plains sites.

The results of this model calculation are compared with measured values in Fig. 4A (Table 3). The C_3 and C_4 data for BLDR, though shown, are excluded from all model regressions because of the suspected influence of the mountains on the source water hydrogen isotope values. The least-squared regression of measured on predicted values has a slope of 0.93 and an intercept of −17.76‰ with an r^2 of 0.42. Four points have more positive measured than predicted values. These are the C_3 and C_4 grasses from the two driest sites, SVL and SGS. These sites are probably more affected by soil evaporation and transpiration than the greenhouse grasses. These points illustrate that the 'direct analog' model fails to explain the isotopic variability of the field samples.

4.4.2. The 'leaf-water' model

This model explicitly considers the isotopic effects of transpiration on leaf-water, which is a function of the temperature and relative humidity of the greenhouse and Great Plains sites. Using a Craig–Gordon type model (Craig and Gordon, 1965), we estimate the expected transpirational D-enrichment in the greenhouse grasses, and calculate new enrichment factors between C_{29} *n*-alkane and bulk leaf-water, $\varepsilon_{C_{29}\text{-BLW}}$. Bulk leaf-water hydrogen isotope values are then modeled for each site and used to calculate $\delta D_{C_{29}}$ using the $\varepsilon_{C_{29}\text{-BLW}}$ estimated from the greenhouse plants.

As discussed above, the long parallel veins and differences in interveinal distance lead to differences in transpirational D-enrichment of leaf-water in C_3 and C_4 grasses (Helliker and Ehleringer, 2000, 2002a,b; Farquhar and Gan, 2003; Gan et al., 2003). These differences can be modeled with analogy to a string-of-lakes model (Gat and Bowser, 1991; Helliker and Ehleringer, 2000) and by considering peclet effects (Farquhar and Gan, 2003; Gan et al., 2003). However, the details of leaf anatomy and evaporative fluxes required for these models are not available for our study. We use the Craig–Gordon model (Craig and Gordon, 1965) as a starting point for estimating transpirational effects (Craig and Gordon, 1965; Farquhar et al., 1989; White, 1989; Flanagan et al., 1991; Roden and Ehleringer, 1999). The Craig–Gordon model characterizes the isotopic effects of evaporation as equilibrium fractionation into saturated air at the air–liquid interface, kinetic fractionation due to diffusion across a humidity gradient, and isotopic exchange between atmospheric water vapor and liquid. In this approach, the hydrogen isotope ratios of leaf-water are influenced only by climate and not by leaf anatomy. As a result, the anatomical differences between C_3 and C_4 grasses are accounted for empirically and implicitly. The enrichment factor between C_{29} *n*-alkane and bulk leaf-water, $\varepsilon_{C_{29}\text{-BLW}}$, includes the isotopic imprint of both the biochemical H-assimilation into lipids and the anatomical contribution to transpirational D-enrichment. Thus, although the biochemical component of the net fractionation in C_3 and C_4 plants may be the same (Flanagan et al., 1991), the modeled $\varepsilon_{C_{29}\text{-BLW}}$ differs by approximately

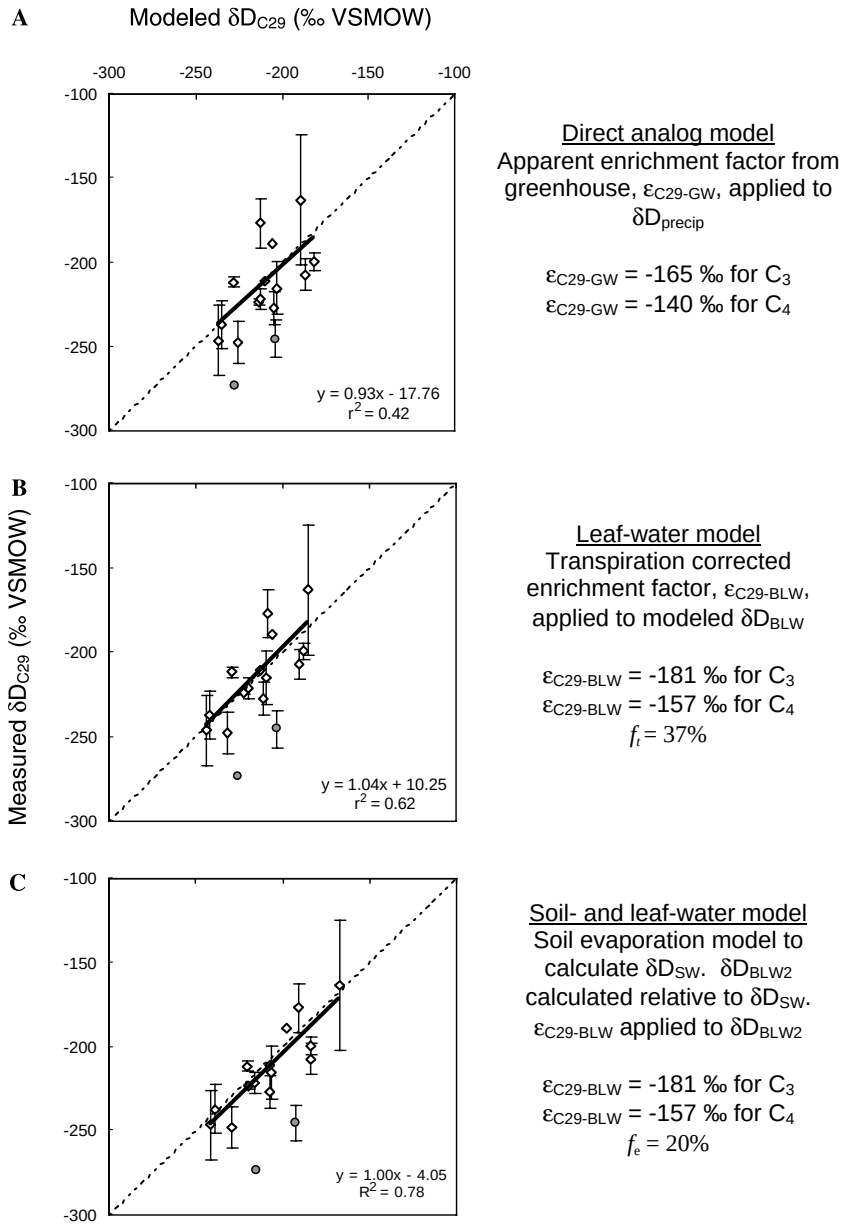

Fig. 4. Comparison of three models with measured δD values for C_{29} *n*-alkane from C_3 and C_4 grasses collected from the Great Plains. Measured values are means for C_3 or C_4 grasses from each site (Table 3). Error bars are ± one standard deviation and reflect isotopic variation among different species at a site. Solid lines and equations represents least squares regressions with the Boulder (BLDR) data (gray circles) excluded. Dashed line represents a 1:1 relationship.

23‰, the difference observed between C_3 and C_4 grasses grown in the greenhouse.

Transpiration can been modeled as evaporation through stomata following the Craig–Gordon model (Craig and Gordon, 1965; Farquhar et al., 1989; White, 1989; Flanagan et al., 1991; Roden and Ehleringer, 1999). Additional terms can be added to describe boundary layer conditions for leaves (Flanagan et al., 1991; Roden and Ehleringer, 1999). However, the addition of these terms only improves hydrogen isotope estimates by 2–5‰ (Flanagan, 1993), which is within our measurement precision. Thus, the simpler model is considered here (Fig. 5). This model calculates the D/H ratio for the transpirationally enriched leaf-water pool (R_{TE}) at isotopic steady state as (Flanagan et al., 1991)

$$R_{TE} = \alpha^*[\alpha_k R_{xylem}((e_i - e_a)/e_i) + R_a(e_a/e_i)], \quad (2)$$

where α^* and α_k are equilibrium and kinetic fractionation factors, respectively; R_{xylem} and R_a are the D/H ratios of xylem water and atmospheric water vapor, respectively; e_i and e_a are the partial pressure of water vapor in intercellular air spaces and the atmosphere. The liquid–vapor equilibrium fractionation factor, α^*, is defined as R_{liquid}/R_{vapor} and is calculated as a function of temperature using the equation of Horita and Wesolowski (1994) (Table 4). The kinetic fractionation, α_k, due to differences in the rate of

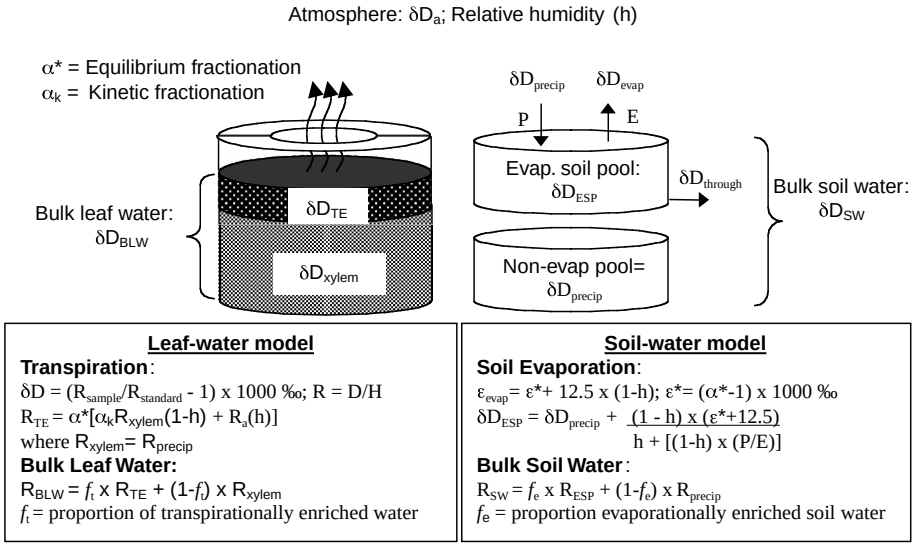

Fig. 5. Schematics describing the leaf- and soil-water models. The leaf-water model (left) describes transpiration through the stomatal opening as a steady state Craig–Gordon type model (Craig and Gordon, 1965) in which the partial pressure of water vapor in the internal air space is assumed to be at saturation vapor pressure. The soil evaporation model is fashioned after through-flow lake model at isotopic and hydrologic steady state (Gat, 1995). In both models, δD_a is assumed to be in isotopic equilibrium with precipitation.

diffusion in air of water vapor containing D versus H has been measured as 1.025 by Merlivat (1978). Because uptake by roots is non-fractionating, the D/H ratio of xylem, R_{xylem}, is assumed to be the same as the plant source water, which in this model is precipitation. The partial pressure of water vapor in intercellular air spaces, e_i, and the ambient atmosphere, e_a, can be related to relative humidity, h, by assuming that the intercellular leaf space is at saturation vapor pressure and at the ambient temperature. Although not always the case, especially in more arid areas, the D/H ratio of atmospheric water vapor, R_a, is assumed to be in isotopic equilibrium with precipitation and thus

$$R_a = R_{precip}/\alpha^*. \quad (3)$$

Eq. (2) can then be rewritten as

$$R_{TE} = \alpha^*[\alpha_k R_{precip}(1-h) + (R_{precip}/\alpha^*)(h)]. \quad (4)$$

This equation is easily related to delta notation by dividing both sides by R_{vsmow} and using the definition of δD (Fig. 5).

Temperatures were obtained from climate stations (State Climatological Summaries from http://nndc.noaa. govget site ref) for each site, or nearby sites for July of the year the samples were collected and relative humidity was estimated from the NCEP-NCAR reanalysis (http://www.cdc.noaa.gov/Composites/) (Table 4). Climate data for July were used because it is frequently the warmest and driest month, and also precedes all of the sample collection dates (Table 4).

The resultant value, δD_{TE}, is for the pool of leaf-water that is transpirationally D-enriched (Table 4). Hydrogen isotope data from leaf-water and -cellulose indicate that water used in cellulose synthesis in grasses is a mixture of xylem water and transpirationally D-enriched water and can be modeled as a mixing of the two (Helliker and Ehleringer, 2002b). The hydrogen isotope ratio of the bulk leaf-water is described as

$$R_{BLW} = f_t \times R_{TE} + (1 - f_t) \times R_{xylem}, \quad (5)$$

where f_t is the fraction derived from transpirationally D-enriched pool. Leaf-water and -cellulose data for C_3 and C_4 grasses suggest a value of 37% for f_t (Helliker and Ehleringer, 2002b) and we use this value to calculate δD_{BLW} (Table 4, Figs. 5 and 6).

Calculating $\delta D_{C_{29}}$ values from modeled δD_{BLW} values requires enrichment factors that account for transpiration. These $\varepsilon_{C_{29}\text{-}BLW}$ values are derived by using the leaf-water model to calculate δD_{BLW} for the greenhouse grasses. Given the greenhouse water composition of $-61.3‰$ and climate (20 °C; $h = 52\%$), the modeled δD_{TE} value for the greenhouse grasses is $-11‰$, and the δD_{BLW} is $-43‰$ (Table 4). Thus, we calculate the fractionation between observed greenhouse values (Table 1) and modeled bulk leaf-water, $\varepsilon_{C_{29}\text{-}BLW}$, to be $-181 \pm 12‰$ for C_3 and $-157 \pm 15‰$ for C_4 grasses (±95% CI).

Using the greenhouse-derived $\varepsilon_{C_{29}\text{-}BLW}$ values, we calculate the $\delta D_{C_{29}}$ values for the field samples relative to modeled bulk leaf-water values (Table 4, Figs. 5 and 6). Comparison of modeled and measured values shows a relationship closer to 1:1 (slope = 1.04, intercept = 10.25) and higher correlation ($r^2 = 0.62$) than the 'direct analog' model (Fig. 4B). The leaf-water model explicitly considers the climatic differences between the field sites and the greenhouse, and therefore, better captures the variability in the field data. Nonetheless, the model still predicts more negative values than observed at the most arid sites, SVL and SGS. The continued underestimation of the $\delta D_{C_{29}}$ for these sites suggests that additional evaporative D-enrichment in soils may be important.

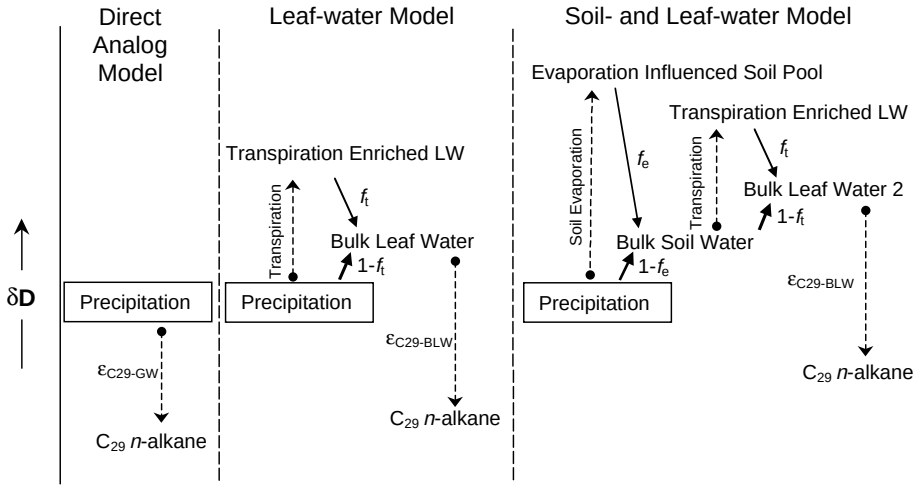

Fig. 6. Conceptual diagram of three models illustrating relative hydrogen isotope compositions.

4.4.3. The 'soil- and leaf-water' model

To examine the potential influence of evaporation from soils, we combine the leaf-water model with a soil-water model based on the lake water models of Gat (1995) (Fig. 5). Soil systems behave differently than open water bodies because of the lack of turbulent vertical mixing and large diffusive sub-layer in unsaturated soils (Barnes and Turner, 1998). As a result, evaporation fronts develop within soils with characteristics that depend on soil properties such as porosity and tortuosity (Barnes and Allison, 1988). Rather than assume soil properties, we have chosen to develop a soil-water model that mimics a soil profile by treating the evaporation front as a through-flow reservoir at hydrologic and isotopic steady state (Gat, 1995). The evaporation-influenced water pool is mixed with non-evaporated water from depth (Figs. 5 and 6). Grasses access water from various depths in the soil profile and thus the soil water they use will represent an isotopic mixture.

The hydrogen isotope ratio of the evaporated soil-water pool (ESP) is modeled as

$$\delta D_{ESP} = \delta D_{precip} + \frac{\delta D_a - \delta D_{precip} + \varepsilon/h}{1 + [(1-h)/h] \times (P/E)}, \quad (6)$$

where δD_{precip} is hydrogen isotope ratio of precipitation; δD_a is hydrogen isotope ratio of atmospheric water vapor; ε is total fractionation (kinetic + equilibrium), between liquid and vapor; h is relative humidity; P is flux of water in via precipitation; E is evaporation flux (Gat, 1995). If we assume that the atmospheric water vapor is in isotopic equilibrium with the precipitation, then

$$\delta D_a = \delta D_{precip} - \varepsilon^*, \quad (7)$$

where ε^* is the equilibrium enrichment factor between liquid and vapor. Kinetic fractionation can be estimated as $12.5\ (1-h)$ (Gonfiantini, 1986). Thus, total fractionation due to evaporation is

$$\varepsilon = \varepsilon^* + 12.5(1-h). \quad (8)$$

Eq. (3) can then be simplified to

$$\delta D_{ESP} = \delta D_{precip} + \frac{(1-h) \times (\varepsilon^* + 12.5)}{h + [(1-h) \times (P/E)]}. \quad (9)$$

The equilibrium enrichment factor between liquid and vapor, ε^*, is calculated from α^* (Horita and Wesolowski, 1994) (Table 4, Fig. 5). The temperature and relative humidity data were the same as those used in the leaf-water model (Table 4). Precipitation and pan evaporation data are from the State Climatological Summaries (http://nndc.noaa.govgetsiteref) for each site, or nearby sites for July of the year the samples were collected (Table 5). Actual evaporation from a lake surface is often observed to be approximately 70% of that measured from an evaporation pan (Gonfiantini, 1986; Gibson and Edwards, 1996; Gibson et al., 1998). Thus, evaporation used in this model is 70% of measured pan evaporation.

The hydrogen isotope ratio of the bulk soil-water is calculated as the mixing of the evaporated soil-water pool with precipitation.

$$R_{SW} = f_e \times R_{ESP} + (1 - f_e) \times R_{precip}, \quad (10)$$

where f_e is the fraction of the soil-water that is derived from the evaporated soil-water pool. The resulting δD_{SW} is then used in the leaf-water model in place of δD_{precip} (Table 5, Figs. 5 and 6). The value for f_e was optimized to produce the best fit between predicted and measured $\delta D_{C_{29}}$. With f_e set to 20%, the relationship between predicted and measured values has a slope of 1.00 and an intercept of −4.05‰, which is within measurement precision of 0, and a squared correlation of 0.78 (Fig. 4C). The two most arid sites, SVL and SGS, show the largest correction by the addition of the soil-water model, suggesting that evaporation from soils is a necessary component for interpreting hydrogen isotope ratios in arid areas.

4.4.4. Model comparison

The model predictions of $\delta D_{C_{29}}$ improve with additions of transpiration and soil evaporation (Fig. 4).

Table 5
Climate data and 'soil- and leaf-water' model calculations of C_{29} *n*-alkane δD (‰ VSMOW)

Site code	July precipitation (mm)[a]	July evaporation (mm)[a]	δD_{ESP}	δD_{SW}[b]	δD_{BLW2}[c]	Soil + leaf-water model C_3 $\delta D_{C_{29}}$[d]	Soil + leaf-water model C_4 $\delta D_{C_{29}}$[d]
WDW[e]	108	180	−63	−81	−74	−242	−219
MNDN	94	200	−57	−79	−70	−239	−216
SDSU	164	244	−46	−68	−59	−229	−206
SGS[f]	58	188	−16	−64	−49	−221	−198
BLDR[g]	50	194	0	−59	−42	−215	−192
KNZA	56	241	−15	−41	−32	−207	−184
HAYS[h]	88	298	−7	−45	−32	−207	−184
SVL	40	263	62	−33	−12	−191	−167

[a] Mean precipitation and pan evaporation from state climatological summaries sites (http://nndc.noaa.gov) for July 1996 (BLDR and SVL) and July 1997 for all other sites.
[b] Bulk soil-water pool with $f_e = 20\%$.
[c] Bulk leaf-water δD_{BLW2} calculated using $\delta D_{xylem} = \delta D_{SW}$, and $f_t = 37\%$ (Figs. 5 and 6).
[d] Calculated using, $\varepsilon_{C_{29}\text{-BLW}}$, of −181‰ for C_3 and −157‰ for C_4.
[e] Evaporation data for WDW not available. Substituted data for Carrington 4N which is 23 miles away.
[f] Precipitation data for 1997 not available for SGS. Substituted data from Greeley, CO, which is 20 miles away. Evaporation data not available for SGS. Substituted data from Fort Collins, CO, which is 15 miles away.
[g] Evaporation data not available for BLDR. Substituted data for Fort Collins, CO, which is 40 miles away.
[h] Evaporation data not available for HAYS. Substituted data for Marion Lake, KS.

Leaf-water isotopic signatures are calculated (leaf-water model) as a function of δD_{precip} values, climate and an f_t value derived from the literature. Without any tuning, the model accounts for over 60% of the variance. The soil-water model was added to determine whether the predictions could be improved significantly by considering an additional evaporative process. The addition of a soil-water model can be optimized to explain nearly 80% of the variance. The ability of the combined soil- and leaf-water models to predict the measured values indicates that climatic influences on the hydrogen isotope ratios of leaf wax *n*-alkanes can be characterized mechanistically.

Relative humidity is the controlling climatic parameter in both the soil- and leaf-water models. Sensitivity tests were performed by varying individual parameters and holding all others constant at the average value for the 8 sites, with f_t set to 37% and f_e set to 20%. Increasing temperature from 21 to 28 °C, which captures the entire range of July temperatures at these sites, only decreases the modeled $\delta D_{C_{29}}$ values by 0.9‰ in the 'leaf-water' model and 1.3‰ in the 'leaf- and soil-water' model. Similarly, increasing the precipitation to evaporation ratio, $P/(70\%E)$, from the minimum to the maximum observed value (0.22–0.96) in the soil-water model only decreases the predicted $\delta D_{C_{29}}$ value by 2‰. In contrast, decreasing relative humidity from 65 to 45%, leads to an increases the modeled $\delta D_{C_{29}}$ values of 6‰ for the 'leaf-water' model and 11‰ for the 'leaf- and soil-water' model. Unlike the 'leaf-water' modeled $\delta D_{C_{29}}$ values that respond linearly to changes in relative humidity, 'leaf- and soil-water' modeled values exhibit a larger response at lower relative humidity. Thus, changes relative humidity in arid areas should have magnified effects on $\delta D_{C_{29}}$ values through soil evaporation.

4.5. Potential paleoclimate proxy

The apparent fractionation between *n*-alkanes and source water differs between C_3 and C_4 grasses, and between grasses and other plant types as seen by the comparison of our results with the data of Chikaraishi and Naraoka (2003) and Sachse et al. (2004a,b). Therefore, any application of hydrogen isotopes in plant compounds in the geologic past will need to account for these differences by characterizing the flora in terms of photosynthetic pathway and plant physiognomic groups, especially during periods when the extent and type of grassland ecosystems might be changing (e.g. Schefuß et al., 2005). This might best be gained through a combination of characterization of the macrofloral and pollen assemblages in conjunction with biomarkers and carbon-isotope analyses of individual plant compounds.

Once the flora is well characterized in terms of the relative importance of dicots, monocots, and C_3 and C_4 grasses, meteoric water δD values could be obtained from δD values of algal biomarkers such as C_{17} *n*-alkane (Huang et al., 2004; Sachse et al., 2004b) from coeval lacustrine deposits. Apparent enrichment factors can be calculated based on these estimated meteoric water δD values. Variation in apparent enrichment factors has been shown here to relate to aridity and could provide a measure of the evaporational conditions experienced at the ecosystem level. The isotopic characterization of grasses performed here is most relevant to grass-dominated ecosystems that are prevalent from the mid-Miocene onward on many continents (Jacobs et al., 1999). Paleohydrologic reconstructions for other terrestrial ecosystems will benefit from additional mechanistic studies of the isotopic variability among different plant types.

5. Conclusions

Hydrogen isotope ratios of *n*-alkanes differ in C_3 and C_4 grasses grown side by side in both the greenhouse and the Great Plains, with C_4 grasses having more positive δD values than C_3 by about 20‰. The most likely cause for this difference is that veins in the leaves of C_4 grasses are closer together than in C_3 grasses, which allows for greater back diffusion of transpirationally enriched water from stomata to veins. Apparent enrichment factors between C_{29} *n*-alkane and greenhouse water ($\varepsilon_{C_{29}\text{-GW}}$) determined from the greenhouse experiments are −165‰ for C_3 and −140‰ for C_4 grasses. However, because transpiration leads to D-enrichment in leaf-water, observed apparent fractionations underestimate actual biochemical fractionation. Application of a simple Craig–Gordon model to account for transpiration provides revised enrichment factors of −181‰ for C_3 and −157‰ for C_4. These enrichment factors are an improved estimate of the fractionation between leaf-water and *n*-alkanes that implicitly and empirically include the effect of differing interveinal distance on transpirational enrichment in C_3 and C_4 grasses.

Comparison of our data for grasses with previous studies (Chikaraishi and Naraoka, 2003; Sachse et al., 2004b) reveals that apparent enrichment factors between *n*-alkanes and meteoric water, $\varepsilon_{\text{lipid–water}}$, are most negative for C_3 grasses, intermediate for C_4 grasses and least negative for C_3 dicots (herbs, shrubs, and trees). Thus, photosynthetic pathway does not control hydrogen isotope fractionation in lipid synthesis. Rather, leaf anatomy and growth form appear to influence hydrogen isotope composition by affecting the degree transpirational enrichment.

Hydrogen isotope ratios of C_{29} *n*-alkanes from Great Plains grasses span 140‰. The northern sites have the most negative values, and the southern sites have the least negative values reflecting the latitudinal precipitation gradient. However, the apparent hydrogen isotope fractionation between precipitation and C_{29} *n*-alkane is not uniform. The dryer sites exhibit smaller absolute apparent fractionation, suggestive of evaporative enrichment through transpiration and/or evaporation from soils. Modeling of the isotopic effects of transpiration and evaporation from soils suggests that both processes are important, and are most sensitive to relative humidity, especially at arid sites. When both are explicitly considered, linear regression of the modeled and measured values has a slope of 1.00 and an intercept of −4.05‰, with an r^2 of 0.78.

Future applications of *n*-alkane δD values as a paleohydrologic proxy will require that the different enrichment factors for C_3 and C_4 grasses, as well as for other plant types, be taken into consideration. If the paleoflora and the meteoric water δD value can be characterized, the hydrogen isotope ratios of leaf-wax *n*-alkanes have great potential to provide a measure of the evaporative enrichment and a paleo-aridity index.

Acknowledgments

We thank Denny Walizer, Pratigya Polissar, Chris Lernihan, and David Beausang for their technical support. Heather Karsten, David Huff, Roy Knupp, and Paul Rebarchack kindly provided access to grass plants for sampling from the greehouses in at Penn State. Thank you to the researchers and staff at the USDA Northern Great Plains Research Laboratory, the Northern Prairie Wildlife Research Center, the SDSU Cottonwood Range and Livestock Research Station, the Shortgrass Steppe LTER, the Konza Prairie LTER, the Fort Hays College Farm, and the Sevilleta LTER for their assistance in the field. We thank the INSTAAR Stable Isotope Lab for analysis of water samples. The manuscript was greatly benefited from thoughtful reviews by Alex Sessions and two anonymous reviewers. This research was supported by an American Chemical Society Grant PRF# 38836-AC2, the Penn State Institutes of the Environment and the Penn State Biogeochemical Research Initiative for Education (BRIE) sponsored by NSF (IGERT) Grant DGE-9972759.

Associate editor: Carol Arnosti

References

Andersen, N., Paul, H.A., Bernasconi, S.M., McKenzie, J.A., Behrens, A., Schaeffer, P., Albrecht, P., 2001. Large and rapid climate variability during the Messinian salinity crisis: evidence from deuterium concentrations of individual biomarkers. *Geology* **29**, 799–802.

Barnes, C.J., Allison, G.B., 1988. Tracing of water movement in the unsaturated zone using stable isotopes of hydrogen and oxygen. *Journal of Hydrology* **100**, 143–176.

Barnes, C.J., Turner, J.V., 1998. Isotopic exchange in soil water. In: Kendall, C., McDonnell, J.J. (Eds.), *Isotope Tracers in Catchment Hydrology*. Elsevier, pp. 137–163.

Bi, X., Sheng, G., Liu, X., Li, C., Fu, J., 2005. Molecular and carbon and hydrogen isotopic composition of *n*-alkanes in plant leaf waxes. *Organic Geochemistry* **36**, 1405–1417.

Boutton, T.W., Archer, S.R., Midwood, A.J., 1999. Stable isotopes in ecosystem science: structure, function and dynamics of a subtropical savanna. *Rapid Communications in Mass Spectrometry* **13**, 1263–1277.

Bowen, G.J., Revenaugh, J., 2003. Interpolating the isotopic composition of modern meteoric precipitation. *Water Resources Research* **39** (10), 1299. doi:10.1029/2003WR002086.

Bowen, G.J., Wilkinson, B., 2002. Spatial distribution of $\delta^{18}O$ in meteoric precipitation. *Geology* **30** (4), 315–318.

Burgoyne, T.W., Hayes, J.M., 1998. Quantitative production of H_2 by pyrolysis of gas chomatographic effluents. *Analytical Chemistry* **70** (24), 5136–5141.

Chikaraishi, Y., Naraoka, H., 2003. Compound-specific δD–$\delta^{13}C$ analyses of *n*-alkanes extracted from terrestrial and aquatic plants. *Phytochemistry* **63**, 361–371.

Chikaraishi, Y., Naraoka, H., Poulson, S.R., 2004. Carbon and hydrogen isotopic fractionation during lipid biosynthesis in a higher plant (*Cryptomeria japonica*). *Phytochemistry* **65**, 323–330.

Collister, J.W., Rieley, G., Stern, B., Eglinton, G., Fry, B., 1994. Compound-specific $\delta^{13}C$ analyses of leaf lipids from plants with differing photosynthetic pathways. *Organic Geochemistry* **21**, 619–627.

Coupland, R.T., 1992. Overview of the grasslands of North America. In: Coupland, R.T. (Ed.), *Natural Grasslands: Introduction and Western Hemisphere*, vol. 8A. Elsevier, pp. 147–149.

Craig, H., 1961. Isotope variations in meteoric water. *Science* **133**, 1702–1703.

Craig, H., Gordon, L.I., 1965. Deuterium and oxygen-18 variations in the ocean and the marine atmosphere. In: Tongiorgi, E. (Ed.), *Proceedings of the Third Spoletto Conference on Stable Isotopes in Oceanographic Studies and Paleotemperatures*. CNR-Laboratorio di Geologia Nucleare, London, pp. 9–130.

Craig, H., Gordon, L.I., Horibe, Y., 1963. Isotopic exchange effects in the evaporation of water. *Journal of Geophysical Research* **68**, 5079–5087.

Dansgaard, W., 1964. Stable isotopes in precipitation. *Tellus* **16**, 436–438.

Dawson, T.E., Mambelli, S., Plamboeck, A.H., Templer, P.H., Tu, K.P., 2002. Stable isotopes in plant ecology. *Annual Review of Ecology and Systematics* **33**, 507–559.

Dawson, T.E., Pausch, R.C., Parker, H.M., 1998. The role of hydrogen and oxygen stable isotopes in understanding water movement along the soil–plant-atmospheric continuum. In: Griffiths, H. (Ed.), *Stable Isotopes: Integration of Biological, Ecological and Geochemical Processes*. Bios Scientific Publishers, pp. 169–183.

Eglinton, G., Hamilton, R.J., 1967. Leaf epicuticular waxes. *Science* **156**, 1322–1334.

Epstein, S., Mayeda, T., 1953. Variation of the O-18 content of waters from natural sources. *Geochimica et Cosmochimica Acta* **5**, 213–224.

Epstein, S., Yapp, C.J., Hall, J.H., 1976. The determination of the D/H ratio of non-exchangeable hydrogen in cellulose extracted from aquatic and land-plants. *Earth and Planetary Science Letters* **30**, 241–251.

Farquhar, G.D., Ehleringer, J.R., Hubick, K.T., 1989. Carbon isotope discrimination in photosynthesis. *Annual Review of Plant Physiology and Plant Molecular Biology* **40**, 503–537.

Farquhar, G.D., Gan, K.S., 2003. On the progressive enrichment of the oxygen isotopic composition of water along a leaf. *Plant Cell and Environment* **26**, 1579–1597.

Flanagan, L.B., 1993. Environmental and biological influence on the stable oxygen and hydrogen isotope composition of leaf water. In: Ehleringer, J.R., Hall, A.E., Farquhar, G.D. (Eds.), *Stable Isotopes in Plant Carbon–Water Relations*. Academic Press, pp. 71–90.

Flanagan, L.B., Comstock, J.P., Ehleringer, J.R., 1991. Comparison of modeled and observed environmental influences on the stable oxygen and hydrogen isotope composition of leaf water in *Phaseolus vulgaris* L.. *Plant Physiology* **96**, 588–596.

Freeman, K.H., Colarusso, L.A., 2001. Molecular and isotopic records of C_4 grassland expansion in the late Miocene. *Geochimica et Cosmochimica Acta* **65** (9), 1439–1454.

Gan, K.S., Wong, S.C., Yong, J.W.H., Farquhar, G.D., 2003. Evaluation of models of leaf water ^{18}O enrichment using measurements of spatial patterns of vein xylem water, leaf water and dry matter in maize leaves. *Plant Cell and Environment* **26**, 1479–1495.

Gat, J.R., 1995. Stable isotopes of fresh and saline lakes. In: Lerman, A., Imboden, D.M., Gat, J.R. (Eds.), *The Physics and Chemistry of Lakes*. Springer-Verlag, pp. 139–164.

Gat, J.R., 1996. Oxygen and hydrogen isotopes in the hydrologic cycle. *Annual Review of Earth and Planetary Sciences* **24**, 225–262.

Gat, J.R., Bowser, C., 1991. The heavy isotope enrichment of water in coupled evaporative systems. In: Taylor, H.P., O'Neil, J.R., Kaplan, I.R. (Eds.), *Stable Isotope Geochemsitry A Tribute to Samuel Epstein*, vol. 3. Geochemical Society.

Gibson, J.J., Edwards, W.T., 1996. Development and validation of an isotopic method for estimating lake evaporation. *Hydrological Processes* **10**, 1369–1382.

Gibson, J.J., Reid, R., Spence, C., 1998. A six-year isotopic record of lake evaporation at a mine site in the Canadian subarctic: results and validation. *Hydrological Processes* **12**, 1779–1792.

Gonfiantini, R., 1986. Environmental isotopes in lake studies. In: Fritz, P., Fontes, T.C. (Eds.), *Handbook of Environmental Isotope Geochemistry*, vol. 2. Elsevier, pp. 112–168.

Harvey, F.E., Welker, J.M., 2000. Stable isotope composition of precipitation in the semi-arid north-central portion of the US Great Plains. *Journal of Hydrology* **238**, 90–109.

Helliker, B.R., Ehleringer, J.R., 2000. Establishing a grassland signature in the veins: ^{18}O in the leaf water of C_3 and C_4 grasses. *Proceedings of the National Academy of Sciences of the United States of America* **97** (14), 7894–7898.

Helliker, B.R., Ehleringer, J.R., 2002a. Differential ^{18}O enrichment of leaf cellulose in C_3 versus C_4 grasses. *Functional Plant Biology* **29**, 435–442.

Helliker, B.R., Ehleringer, J.R., 2002b. Grass blades as tree rings: environmentally induced changes in the oxygen isotope ratio of cellulose along the length of grass blades. *New Phytologist* **155**, 417–424.

Hilkert, A.W., Douthitt, C.B., Schlüter, H.J., Brand, W.A., 1999. Isotope ratio monitoring gas chromatography/mass spectrometry of D/H by high temperature conversion isotope ratio mass spectrometry. *Rapid Communications in Mass Spectrometry* **13**, 1226–1230.

Horita, J., Wesolowski, D.J., 1994. Liquid–vapor fractionation of oxygen and hydrogen isotopes of water from the freezing to the critical temperature. *Geochimica et Cosmochimica Acta* **58** (16), 3425–3437.

Huang, Y., Dupont, L., Sarnthein, M., Hayes, J.M., Eglinton, G., 2000. Mapping of C_4 input from North West Africa into North East Atlantic sediments. *Geochimica et Cosmochimica Acta* **64**, 3505–3513.

Huang, Y., Shuman, B., Wang, Y., Webb Jr., T., 2002. Hydrogen isotope ratios of palmitic acid in lacustrine sediments record late Quaternary climate variations. *Geology* **30** (12), 1103–1106.

Huang, Y., Shuman, B., Wang, Y., Webb Jr., T., 2004. Hydrogen isotope ratios of individual lipids in lake sediments as novel tracers of climatic and environmental change: a surface sediment test. *Journal of Paleolimnology* **31**, 363–375.

Huang, Y., Street-Perrott, F.A., Metcalfe, S.E., Brenner, M., Moreland, M., Freeman, K.H., 2001. Climate change as the dominant control on glacial–interglacial variations in the C_3 and C_4 plant abundance. *Science* **293**, 1647–1651.

IAEA. 2001. GNIP Maps and Animations, International Atomic Energy Agency, Vienna. Accessible from: <http://isohis.iaea.org>.

Ingraham, N.L., 1998. Isotopic variations in precipitation. In: Kendall, C., McDonnell, J.J. (Eds.), *Isotope Tracers in Catchment Hydrology*. Elsevier, pp. 87–118.

Jacobs, B.F., Kingston, J.D., Jacobs, L.L., 1999. The origin of grass-dominated ecosystems. *Annals of the Missouri Botanical Garden* **86**, 590–643.

Kendall, C., Coplen, T.B., 2001. Distribution of oxygen-18 and deuterium in river waters across the United States. *Hydrological Processes* **15**, 1363–1393.

Larcher, W., 1995. *Physiological Plant Ecology*. Springer, pp. 506.

Merlivat, L., 1978. Molecular diffusivities of $H_2{}^{18}O$ in gases. *Journal of Chemical Physics* **69**, 2864–2871.

Northfelt, D.W., DeNiro, M.J., Epstein, S., 1981. Hydrogen and carbon isotopic ratios of the cellulose nitrate and saponifiable lipid fractions prepared from annual growth rings of a California redwood. *Geochimica et Cosmochimica Acta* **45**, 1895–1898.

Pedentchouk, N., 2004. Lacustrine Paleoenvironments from Stable Isotopes of Hydrogen and Carbon in Lipids. Ph.D. dissertation, Pennsylvania State University, 175 p.

Roden, J.S., Ehleringer, J.R., 1999. Observations of hydrogen and oxygen isotopes in leaf water confirm the Craig–Gordon model under wide-ranging environmental conditions. *Plant Physiology* **120**, 1165–1173.

Rozanski, K., Araguás-Araguás, L., Gonfiantini, R., 1993. Isotopic patterns in modern precipitation. In: Swart, P.K., Lohmann, K.C., McKenzie, J., Savin, S. (Eds.), *Climate Change in Continental Isotope Records*, vol. 78. American Geophysical Union, pp. 1–36.

Sachse, D., Radke, J., Gaupp, R., Schwark, L., Lüniger, G., Gleixner, G., 2004a. Reconstruction of paleohydrological conditions in a lagoon during the 2nd Zechstein cycle through simultaneous use of δD values of individual *n*-alkanes and $\delta^{18}O$ and $\delta^{13}C$ values of carbonates. *International Journal of Earth Science* **93**, 554–564.

Sachse, D., Radke, J., Gleixner, G., 2004b. Hydrogen isotope ratios of recent lacustrine sedimentary *n*-alkanes record modern climate variability. *Geochimica et Cosmochimica Acta* **68**, 4877–4889.

Sauer, P.E., Eglinton, T.I., Hayes, J.M., Schimmelmann, A., Sessions, A.L., 2001. Compound-specific D/H ratios of lipid biomarkers from sediments as a proxy for environmental and climatic conditions. *Geochimica et Cosmochimica Acta* **65**, 213–222.

Schefuß, E., Schouten, S., Schneider, R.R., 2005. Climatic controls on central African hydrology during the past 20,000 years. *Nature* **437**, 1003–1006.

Schimmelmann, A., Lewan, M.D., Wintsch, R.P., 1999. D/H isotope ratios of kerogen, bitumen, oil and water in hydrous pyrolysis of source rocks containing kerogen type I, II, IIs and III. *Geochimica et Cosmochimica Acta* **63**, 3751–3766.

Sessions, A.L., Burgoyne, T.W., Hayes, J.M., 2001. Determination of the H_3 factor in hydrogen isotope ratio monitoring mass spectrometry. *Analytical Chemistry* **73**, 200–207.

Sessions, A.L., Burgoyne, T.W., Schimmelmann, A., Hayes, J.M., 1999. Fractionation of hydrogen isotopes in lipid biosynthesis. *Organic Geochemistry* **30**, 1193–1200.

Sessions, A.L., Sylva, S.P., Summons, R.E., Hayes, J.M., 2004. Isotopic exchange of carbon-bound hydrogen over geologic timescales. *Geochimica et Cosmochimica Acta* **68**, 1545–1559.

Shu, Y., Feng, X., Gazis, C., Anderson, D., Faiia, A.M., Tang, K., Ettl, G.J., 2005. Relative humidity recorded in tree rings: a study along a precipitation gradient in the Olympic Mountains, Washington, USA. *Geochimica et Cosmochimica Acta* **69** (4), 791–799.

Simioni, G., Le Roux, X., Gignoux, J., Walcroft, A.S., 2004. Leaf gas exchange characteristics and water- and nitrogen-use efficiencies of dominant grass and tree species in a West African savanna. *Plant Ecology* **173**, 233–246.

Smith, F.A., White, J.W.C., 2004. Modern calibration of phytolith carbon isotope signatures for C_3/C_4 paleograssland reconstruction. *Palaeogeography, Palaeoclimatology, Palaeoecology* **207**, 277–304.

Sternberg, L.S.L., 1988. D/H ratios of environmental water recorded by D/H ratios of plant lipids. *Nature* **333**, 59–61.

Sternberg, L.S.L., DeNiro, M.J., Ajie, H., 1984. Stable hydrogen isotope ratios of saponifiable lipids and cellulose nitrate from CAM, C_3 and C_4 plants. *Phytochemistry* **23** (11), 2475–2477.

Tang, K., Feng, X., 2001. The effect of soil hydrology on the oxygen and hydrogen isotopic composition of plants' source water. *Earth and Planetary Science Letters* **185**, 355–367.

Vaughn, B.H., White, J.W.C., Delmotte, M., Trolier, M., Cattani, O., Stievenard, M., 1998. An automated system for hydrogen isotope analysis of water. *Chemical Geology* **152**, 309–319.

Welker, J.M., 2000. Isotopic ($\delta^{18}O$) characteristics of weekly precipitation collected across the USA: an initial analysis with application to water source studies. *Hydrological Processes* **14**, 1449–1464.

White, J.W.C., 1989. Stable hydrogen isotope ratios in plants: a review of current theory and some potential applications. In: Rundel, P.W., Ehleringer, J.R., Nagy, K.A. (Eds.), *Stable Isotopes in Ecological Research*. Springer Verlag, pp. 143–162.

White, J.W.C., Cook, E.R., Lawrence, J.R., Broecker, W.S., 1985. The D/H ratio of sap in trees: implications for water sources and tree ring D/H ratios. *Geochimica et Cosmochimica Acta* **49**, 237–246.

Xie, S., Nott, C.J., Avsejs, L.A., Volders, F., Maddy, D., Chambers, F.M., Gledhill, A., Carter, J.F., Evershed, R.P., 2000. Paleoclimate records in compound-specific δD values of a lipid biomarker in ombotrophic peat. *Organic Geochemistry* **31**, 1053–1057.

Yamada, K., Ishiwatari, R., 1999. Carbon isotopic composition of long-chain *n*-alkanes in the Japan Sea sediments: implications for paleoenvironmental changes over the past 85 kyr. *Organic Geochemistry* **30**, 367–377.

Yang, H., Huang, Y., 2003. Preservation of lipid hydrogen isotope ratios in Miocene lacustrine sediments and plant fossils at Clarkia, northern Idaho, USA. *Organic Geochemistry* **34**, 413–423.

Yapp, C.J., Epstein, S., 1982. A reexamination of cellulose carbon-bound hydrogen δD measurements and some factors affecting plant-water D/H relationships. *Geochimica et Cosmochimica Acta* **46**, 955–965.

Zhao, M., Eglinton, G., Haslett, S.K., Jordan, R.W., Sarnthein, M., Zhang, Z., 2000. Marine and terrestrial biomarker records for the last 35,000 years at ODP site 658C off NW Africa. *Organic Geochemistry* **31**, 919–930.

Ziegler, H., 1989. Hydrogen isotope Fractionation in plant tissues. In: Rundel, P.W., Ehleringer, J.R., Nagy, K.A. (Eds.), *Stable Isotopes in Ecological Research*. Springer Verlag, pp. 105–123.